Journal of Molecular Spectroscopy **196,** 235–247 (1999)
Article ID jmsp.1999.7886, available online at http://www.idealibrary.com on IDEAL®

Fourier Transform Emission Spectroscopy of the $[7.3]^2\Delta$–$a^2\Phi$ and $[9.4]^2\Phi$-$a^2\Phi$ Systems of ZrCl

R. S. Ram* and P. F. Bernath*,†

*Department of Chemistry, University of Arizona, Tucson, Arizona 85721; and †Department of Chemistry, University of Waterloo, Waterloo, Ontario, Canada N2L 3G1.

Received March 4, 1999; in revised form April 22, 1999

The emission spectrum of ZrCl has been observed in the 1800–12 000 cm^{-1} region using a Fourier transform spectrometer. The molecules were excited in a microwave discharge of a mixture of helium and a trace of $ZrCl_4$ vapor. In addition to the $C^4\Delta$–$X^4\Phi$ transition reported previously, numerous new bands observed in the near infrared have been classified into two electronic transitions, $[7.3]^2\Delta$–$a^2\Phi$ and $[9.4]^2\Phi$–$a^2\Phi$. Five new bands observed in the 6700–7400 cm^{-1} region have been assigned as $^2\Delta_{3/2}$–$^2\Phi_{5/2}$ and $^2\Delta_{5/2}$–$^2\Phi_{7/2}$ subbands of a new electronic transition, $[7.3]^2\Delta$–$a^2\Phi$. The two subbands of the $[9.4]^2\Phi$–$a^2\Phi$ transition were previously observed by G. Phillips, S. P. Davis, and D. C. Galehouse [*Astrophys. J. Suppl.* **43**, 417–434 (1980)], who tentatively labeled them as $^2\Pi_{1/2}$–$^2\Pi_{1/2}$ and $^2\Pi_{3/2}$–$^2\Pi_{3/2}$ subbands. A number of new bands involving higher vibrational levels have been identified for these two subbands. A rotational analysis of a number of bands of both transitions has been obtained and spectroscopic constants have been determined. Global perturbations have been observed in both spin components of the $a^2\Phi$ state. The assignment of the observed electronic states has been discussed in light of recent theoretical calculations.

INTRODUCTION

Although the electronic spectra of ZrCl have been known for several decades (*1*), the identity of the ground state has always been in question. A $^4\Sigma^-$ ground state was suggested on the basis of a vibrational analysis of ZrCl bands observed in the 400–415 nm region by radio frequency excitation of $ZrCl_4$ vapor (*1*). These bands were reinvestigated by Jordan *et al.* (*2*) using a corona-excited supersonic jet source. They classified these bands into four subbands of a $^4\Pi$-$^4\Sigma^-$ transition with the $^4\Sigma^-$ state assigned as the ground state, although no rotational analysis was carried out. The 400–415 nm bands probably belongs to a $^4\Gamma$–$^4\Phi$ system, by analogy with recent work on TiCl (*3*). Phillips *et al.* (*4*) have observed another transition of ZrCl in the near infrared, which was assigned as a $\Delta\Omega = 0$ doublet–doublet transition. Again no conclusion was drawn about the nature of the ground state, although a $^2\Pi$ or $^2\Delta$ assignment was proposed for the lower and upper excited states of this transition.

Recently we have investigated the electronic spectra of ZrCl in the 3000–10 000 cm^{-1} region. We have observed a new transition of ZrCl in the 3600–4400 cm^{-1} region which has been assigned as the $C^4\Delta$–$X^4\Phi$ transition (*5*). The $^4\Phi$ ground state assignment for ZrCl is consistent with our recent findings for TiCl (*6*) and TiF (*7*) and is also consistent with recent *ab initio* results for TiF (*8*). A high-level *ab initio* study of TiF has been carried out by Harrison (*8*), who calculated the spectroscopic properties of a number of doublet and quartet states. This work predicts a $^4\Phi$ state as the ground state consistent with the results of TiH (*9-11*). According to this calculation, the ground state of TiF is followed by a close-lying $^4\Sigma^-$ state about 0.1 eV above the $X^4\Phi$ state and the lowest doublet state is a $^2\Phi$ state which lies about 0.65 eV above the ground $^4\Phi$ state. Similar electronic structure is also expected for the TiCl and ZrCl molecules. The *ab initio* calculations of Boldyrev and Simons (*12*) support the $^4\Phi$ assignment of the ground state for both TiF and TiCl.

Recently Focsa *et al.* have calculated the spectroscopic properties of the low-lying electronic states of TiCl (*13*) and ZrCl (*14*) using ligand field theory. These calculations have also confirmed our assignment of the $^4\Phi$ ground state and have predicted the location of other low-lying doublet and quartet states. A $^2\Phi$ state has been predicted to be the lowest in the doublet manifold of states. Recently we have observed a doublet–doublet transition of TiCl in the near infrared which has been labeled as the $[12.8]^2\Phi$–$a^2\Phi$ transition (*15*). The assignment of the lower state as $a^2\Phi$ is also supported by the calculations of Focsa *et al.* (*13*) for TiCl, but we cannot rule out a $[12.8]^2\Delta$–$a^2\Delta$ assignment. The infrared transition of ZrCl, reported initially by Phillips *et al.* (*4*) is analogous to the $[12.8]^2\Phi$–$a^2\Phi$ transition of TiCl (*15*). This transition has been renamed as the $[9.4]^2\Phi$–$a^2\Phi$ transition in the present paper.

In our recent work on the near-infrared spectra of ZrCl (*5*) we noted that several weaker bands remained unassigned. In this paper we report on the analysis of numerous such bands in the 6700–12 000 cm^{-1} region. Several new bands observed in the 7700–12 000 cm^{-1} region have been identified as higher vibrational bands of the transition initially analyzed by Phillips *et al.* (*4*). In addition, another low-lying transition, $[7.3]^2\Delta$–$a^2\Phi$, with a common lower state has been observed in the

0022-2852/99 $30.00

6700–7400 cm^{-1} region. The rotational analysis of these two transitions will be reported in this paper and the nature of the observed electronic states will be discussed in light of the available theoretical calculations.

EXPERIMENTAL DETAILS

The experimental conditions and methods of observation of the ZrCl bands have been provided in detail in our previous paper (*5*). In summary, the ZrCl molecules were excited in a microwave discharge through a flowing mixture of about 3 Torr of helium and a trace of $ZrCl_4$ vapor. The spectra were recorded using the 1-m Fourier transform spectrometer of the National Solar Observatory at Kitt Peak. The spectra in the 1800–9000 cm^{-1} region were recorded using liquid-nitrogen-cooled InSb detectors and Si filters. A total of 10 scans were co-added in about 60 min of integration at a resolution of 0.02 cm^{-1}.

The spectral line positions were measured using a data reduction program called PC-DECOMP developed by J. Brault. The peak positions were determined by fitting a Voigt lineshape function to each line. The ZrCl bands in the 9000–12 000 cm^{-1} region were measured from the spectra used by Phillips *et al.* (*4*) in their previous study of this molecule. Since no molecular or atomic lines suitable for calibration were present in the 9000–12 000 cm^{-1} region, the sharp atomic lines common to both the spectra were first calibrated using the measurements of the vibration–rotation lines of the 1–0 band of HCl (*16*) which appear in our spectra. This calibration was then transferred to the spectra in the 9000–12 000 cm^{-1} region. All of the bands observed in the 9000–12 000 cm^{-1} region including those reported in the paper of Phillips *et al.* (*4*) were remeasured. There is excellent agreement between the present measurements and those of Phillips *et al.* (*4*). A maximum deviation of ± 0.002 cm^{-1} has been observed between the two sets of measurements. The molecular lines appear with a width of 0.035 cm^{-1} and a maximum signal-to-noise ratio of about 13:1. The line positions are expected to be accurate to about ± 0.003 cm^{-1}. However, because there is considerable overlapping and blending caused by the presence of different subbands in the same region, the error in the measurement of blended and weak lines is expected to be somewhat higher.

OBSERVATIONS AND ANALYSIS

In addition to the $C^4\Delta$–$X^4\Phi$ transition of ZrCl reported previously, numerous additional bands have been observed in our spectra in the 6700–12 000 cm^{-1} region. Most of these bands have been assigned as involving doublet–doublet transitions. The electronic assignment of these transitions has been made with the help of recent theoretical predictions for TiCl (*13*) and ZrCl (*14*). A schematic energy level diagram of the observed doublet–doublet transitions is provided in Fig. 1.

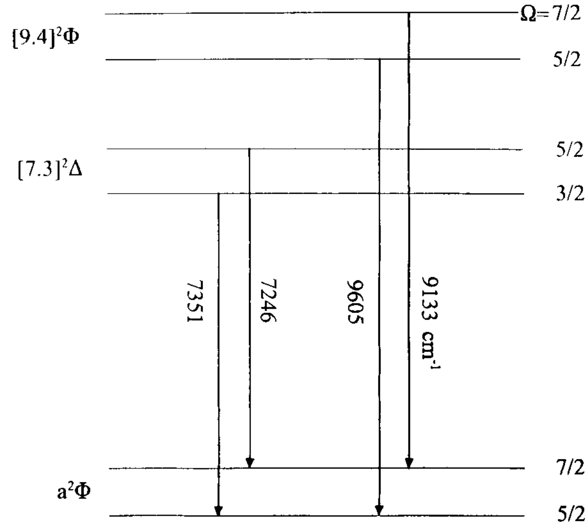

FIG. 1. A schematic energy level diagram of the observed doublet states of ZrCl.

A number of bands observed in the 8000–12 000 cm^{-1} region have been assigned previously by Phillips *et al.* (*4*) into two doublet–doublet subbands with the 0–0 origins near 9133 and 9605 cm^{-1}, respectively. These two subbands were labeled as $^2\Pi_{1/2}$–$^2\Pi_{1/2}$ and $^2\Pi_{3/2}$-$^2\Pi_{3/2}$ transitions (*4*). In the present paper we have renamed this transition as $[9.4]^2\Phi$–$a^2\Phi$ based on a recent theoretical calculation (*14*) and experimental observations on the isovalent TiCl in the 10 000–13 000 cm^{-1} region (*15*). The number quoted in square brackets is the average of the T_{00} values of the two subbands in units of 1000 cm^{-1}. The two $\Delta\Omega = 0$ transitions of ZrCl (*4*) are thus the $[9.4]^2\Phi_{5/2}$–$a^2\Phi_{5/2}$ and $[9.4]^2\Phi_{7/2}$–$a^2\Phi_{7/2}$ subbands.

Several of the bands in the 7000–8700 cm^{-1} region were assigned as higher vibrational bands in the $\Delta v = -2$ and -3 sequences of the $[9.4]^2\Phi$–$a^2\Phi$ transition. In addition, five new bands observed in the 6700–7400 cm^{-1} region have been assigned as two subbands of a new doublet–doublet transition with $\Delta\Omega = \pm 1$. These bands are much weaker in intensity than the bands of Phillips *et al.* (*4*) but involve the same lower state. This transition has been labeled as $[7.3]^2\Delta$–$a^2\Phi$ in the present paper.

(a) The $[9.4]^2\Phi$–$a^2\Phi$ Transition

Phillips *et al.* (*4*) assigned three bands located near 8721, 9133, and 9487 cm^{-1} as the 0–1, 0–0, and 1–0 bands, respectively, of the $^2\Pi_{1/2}$-$^2\Pi_{1/2}$ subband [present notation, $[9.4]^2\Phi_{7/2}$–$a^2\Phi_{7/2}$] and seven ZrCl bands near 8730, 8785, 9195, 9605, 9957, 10 246, and 10 309 cm^{-1} as the 1–3, 0–2, 0–1, 0–0, 1–0, 3–1, and 2–0 bands, respectively, of the $^2\Pi_{3/2}$–$^2\Pi_{3/2}$ subband [present notation, $[9.4]^2\Phi_{5/2}$–$a^2\Phi_{5/2}$]. In the present work we have extended the previous observations to include bands involving higher vibrational levels of the lower and excited states. In particular the new bands observed near 9838, 9776, 8315, 8257, 7855 and 7806 cm^{-1} have been assigned as

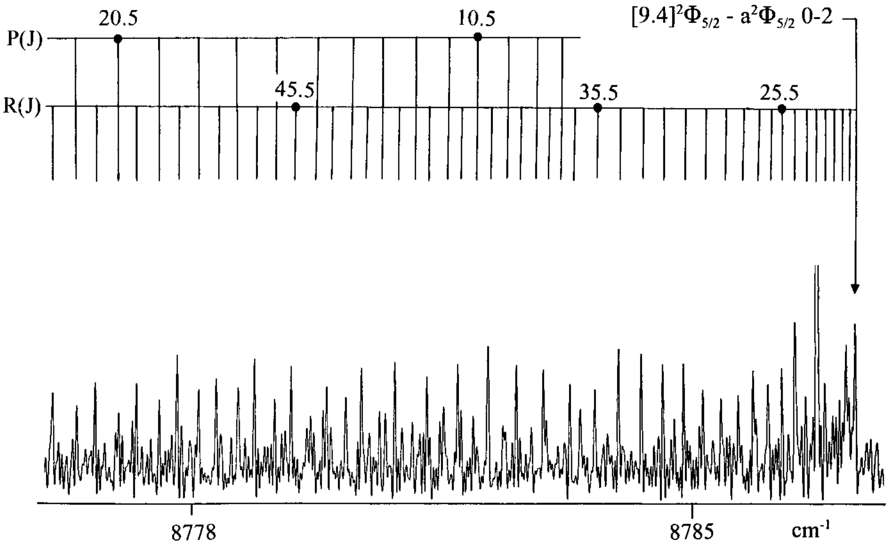

FIG. 2. An expanded portion of the 0–2 band of the $[9.4]^2\Phi_{5/2}$–$a^2\Phi_{5/2}$ subband of ZrCl.

2–0, 3–1, 0–2, 1–3, 1–4 and 2–5 bands of the $[9.4]^2\Phi_{7/2}$–$a^2\Phi_{7/2}$ subband and the bands observed near 9137, 8727, 8375, 8323 cm^{-1} have been assigned as the 1–2, 1–3, 0–3 and 1–4 bands of the $[9.4]^2\Phi_{5/2}$–$a^2\Phi_{5/2}$ subband. All of these new bands have been rotationally analyzed. The rotational structure of each subband consists of two branches: one *R* and one *P*, along with the isotopic companions involving ^{37}Cl and various isotopes of Zr. The rotational structure of the 0–2 band of the $[9.4]^2\Phi_{5/2}$–$a^2\Phi_{5/2}$ subband is provided in Fig. 2, where only the lines of the most abundant ^{90}Zr^{35}Cl isotopomer have been marked. The unmarked lines are due to the less abundant isotopomers involving ^{91}Zr (11.2%), ^{92}Zr (17.2%), ^{94}Zr (17.4%), ^{96}Zr (2.7%), or ^{37}Cl (24.2%) isotopes. No Ω-doubling was observed in any of the bands. The rotational constants for only the most abundant ^{90}Zr^{35}Cl isotopomer have been obtained. The relative size of the B_{eff} values was used to distinguish between the $^2\Phi_{7/2}$ and $^2\Phi_{5/2}$ spin components because first lines were not detected. The observed states have been assigned as regular as suggested by the calculations of Focsa *et al.* (*13,14*) [Fig. 1].

(b) The $[7.3]^2\Delta$–$a^2\Phi$ transition

On the lower wavenumber side of the $[9.4]^2\Phi$–$a^2\Phi$ transition, several weaker bands with *R* heads near 6835, 6940, 7246, 7351, and 7714 cm^{-1} could not be accommodated into the Deslandres table of the two subbands described previously. A careful inspection of the rotational structure of these bands indicates that they have strong *Q* branches and, therefore, involve $\Delta\Omega = \pm 1$ transitions. A rotational analysis of the bands near 6835 and 7246 cm^{-1} indicates that they are the 0–1 and 0–0 bands of a new subband with the $a^2\Phi_{7/2}$ spin component as its lower state, while the bands near 6940, 7351, and

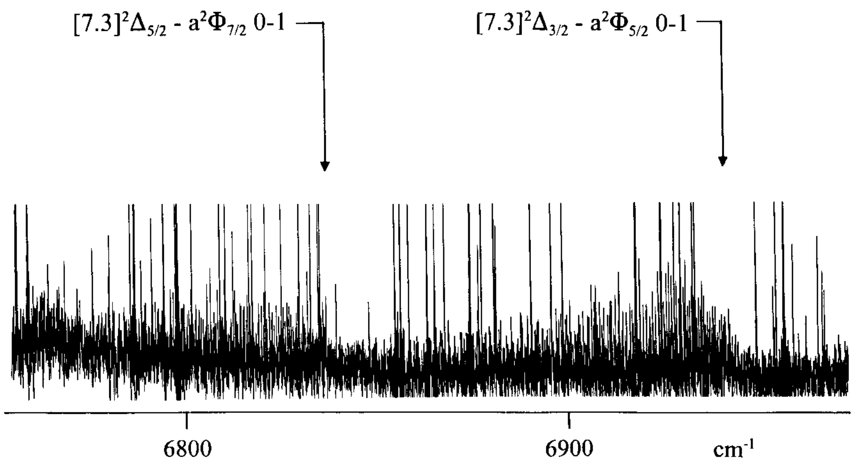

FIG. 3. A compressed portion of the 0–1 band of the $[7.3]^2\Delta_{5/2}$–$a^2\Phi_{7/2}$ and $[7.3]^2\Delta_{3/2}$–$a^2\Phi_{5/2}$ subbands of ZrCl.

TABLE 1

Observed Line Positions (in cm^{-1}) for the New Bands of the $[9.4]^2\Phi$–$a^2\Phi$ System of ZrCl

J	R(J)	Δν	P(J)	Δν	R(J)	Δν	P(J)	Δν	R(J)	Δν	P(J)	Δν
	$[9.4]^2\Phi_{7/2}$ - $a^2\Phi_{7/2}$ 0-2				$[9.4]^2\Phi_{7/2}$ - $a^2\Phi_{7/2}$ 1-3				$[9.4]^2\Phi_{7/2}$ - $a^2\Phi_{7/2}$ 1-4			
13.5											7850.390	-6
14.5											7849.942	-5
15.5											7849.472	-10
16.5											7849.001	-3
17.5											7848.502	-9
18.5											7847.996	-7
19.5											7847.474	-6
20.5	8316.642	11									7846.945	2
21.5	8316.562	3			8258.507	-20					7846.388	-3
22.5	8316.479	5			8258.419	-19					7845.824	0
23.5	8316.372	-4			8258.326	-8					7845.238	-5
24.5					8258.203	-13			7856.486	-4	7844.639	-8
25.5	8316.123	-13			8258.074	-8	8245.759	-6	7856.350	-3	7844.034	-2
26.5			8303.158	10	8257.926	-6	8245.138	-4	7856.203	3	7843.417	7
27.5	8315.840	-4	8302.519	-1	8257.777	9	8244.501	-4	7856.028	-5	7842.770	-0
28.5	8315.676	-2	8301.877	-2	8257.580	-9	8243.849	-3	7855.850	-2	7842.113	-2
29.5	8315.500	-0	8301.230	3	8257.394	1			7855.648	-7	7841.443	-2
30.5	8315.306	-4	8300.558	-3	8257.181	-1	8242.501	1	7855.445	2	7840.756	-5
31.5	8315.112	3	8299.880	-5	8256.957	2			7855.223	6	7840.069	7
32.5	8314.891	-4	8299.193	-4	8256.715	2	8241.084	-1	7854.974	-1	7839.353	5
33.5	8314.678	6	8298.500	1	8256.462	7	8240.358	2	7854.722	3	7838.622	3
34.5	8314.438	0	8297.791	1	8256.192	10	8239.610	1	7854.453	5	7837.875	-2
35.5	8314.196	2	8297.079	7	8255.898	7	8238.828	-19	7854.164	1	7837.109	-9
36.5	8313.945	4	8296.348	4	8255.591	5	8238.071	3	7853.864	2		
37.5	8313.678	-3	8295.612	3	8255.269	5	8237.279	5	7853.562	15	7835.560	2
38.5	8313.407	-5	8294.869	2	8254.931	5	8236.472	8	7853.215	-2	7834.758	3
39.5	8313.149	12	8294.124	6			8235.643	4	7852.879	7	7833.938	-0
40.5	8312.853	-4	8293.372	8	8254.206	5			7852.515	4	7833.113	7
41.5			8292.610	5	8253.813	-1			7852.146	10	7832.263	4
42.5	8312.279	-5	8291.847	5	8253.413	1	8233.061	-2	7851.750	4	7831.400	3
43.5	8311.992	-0	8291.076	-1	8252.989	-3	8232.172	1	7851.351	9	7830.526	4
44.5	8311.710	9	8290.311	-1	8252.559	3	8231.263	-0	7850.927	4	7829.633	2
45.5	8311.403	-7	8289.543	-3	8252.107	5	8230.338	-1	7850.485	-2	7828.730	6
46.5	8311.116	-4	8288.783	-1	8251.636	3	8229.400	2	7850.040	2	7827.806	3
47.5	8310.832	-1	8288.024	1	8251.134	-13	8228.439	-1	7849.573	-0	7826.869	1
48.5	8310.553	1	8287.271	1	8250.646	3	8227.463	-3	7849.094	0	7825.928	11
49.5	8310.273	-4	8286.525	3	8250.118	-5	8226.474	-1	7848.600	1	7824.960	9
50.5	8309.995	-17	8285.786	3	8249.581	-5	8225.463	-5	7848.090	1	7823.974	3
51.5	8309.753	-4	8285.056	1	8249.026	-7	8224.443	-1	7847.566	2	7822.982	7
52.5	8309.513	-1	8284.350	10	8248.455	-7	8223.401	-2	7847.024	-0	7821.965	1
53.5			8283.654	13	8247.868	-7	8222.347	1	7846.473	3	7820.946	6
54.5					8247.261	-9	8221.271	0	7845.901	2	7819.902	3
55.5					8246.646	-3	8220.177	-2	7845.311	-3	7818.843	-1
56.5					8246.006	-4	8219.069	-2	7844.716	2	7817.774	0
57.5					8245.351	-4	8217.940	-6	7844.097	-1	7816.685	-3
58.5					8244.681	-2	8216.802	-2	7843.468	0	7815.591	2
59.5					8243.995	2	8215.641	-3	7842.826	4	7814.471	-3
60.5					8243.286	-0	8214.474	5	7842.161	-0	7813.344	1
61.5					8242.569	5	8213.276	-0	7841.476	-9	7812.194	-4
62.5					8241.814	-9			7840.792	-2	7811.033	-5
63.5											7809.859	-3
64.5					8240.296	3					7808.656	-16
65.5					8239.512	10	8208.367	27			7807.464	-3
66.5					8238.704	9	8207.081	17			7806.240	-6
67.5					8237.878	7	8205.770	-3			7805.009	-1
68.5					8237.036	5	8204.480	16	7836.323	-3	7803.751	-8
69.5					8236.187	13	8203.153	13	7835.505	-23	7802.492	-1
70.5					8235.306	4	8201.804	4	7834.708	-6		
71.5					8234.425	13	8200.442	-2	7833.881	-3	7799.912	-4
72.5					8233.522	14	8199.067	-5	7833.030	-11	7798.594	-10
73.5					8232.588	0			7832.177	-3	7797.275	-2
74.5					8231.652	1	8196.273	-8	7831.295	-10	7795.930	-5
75.5					8230.696	-4	8194.855	-7	7830.407	-7	7794.570	-8
76.5							8193.413	-16	7829.503	-5	7793.199	-6
77.5									7828.599	12	7791.811	-5

Note. Δν's are observed minus calculated wavenumbers in the units of 10^{-3} cm^{-1}.

TABLE 1—*Continued*

J	R(J)	Δν	P(J)	Δν	R(J)	Δν	P(J)	Δν	R(J)	Δν	P(J)	Δν
78.5									7827.656	7	7790.412	-2
79.5									7826.693	-4	7788.989	-5
80.5									7825.750	22	7787.569	8
81.5									7824.748	4	7786.115	4
82.5									7823.745	1	7784.647	0
83.5									7822.740	11	7783.168	2
84.5									7821.711	13	7781.690	19
85.5											7780.170	10
86.5											7778.647	14
87.5											7777.108	17
88.5											7775.553	19
89.5											7773.975	15
	$[9.4]^2\Phi_{7/2}$ - $a^2\Phi_{7/2}$ 2-0				$[9.4]^2\Phi_{7/2}$ - $a^2\Phi_{7/2}$ 2-5				$[9.4]^2\Phi_{7/2}$ - $a^2\Phi_{7/2}$ 3-1			
3.5	9839.308	-2										
4.5	9839.452	-2										
5.5	9839.573	-6										
6.5	9839.684	0	9836.376	-4								
7.5			9836.001	8								
8.5			9835.588	3			7803.321	-12			9773.302	-4
9.5			9835.158	1			7802.955	-2			9772.884	5
10.5			9834.720	11			7802.557	-8			9772.425	-7
11.5							7802.158	-1			9771.968	3
12.5	9839.893	8	9833.756	5			7801.724	-14			9771.499	22
13.5	9839.838	-10	9833.248	5			7801.299	-3	9777.534	-10	9770.961	-8
14.5	9839.791	1	9832.721	7			7800.845	-5	9777.487	2	9770.440	-1
15.5			9832.163	-1	7807.923	-10	7800.381	-4	9777.395	-11	9769.880	-13
16.5	9839.604	-10	9831.593	-1			7799.912	8	9777.296	-11	9769.327	3
17.5	9839.493	-3	9831.006	1			7799.399	-10	9777.195	8	9768.733	-2
18.5	9839.353	-5	9830.397	2			7798.902	3	9777.035	-13	9768.128	2
19.5	9839.204	5	9829.760	-4			7798.376	2	9776.889	2	9767.511	14
20.5			9829.113	-1			7797.835	2	9776.703	-4	9766.850	3
21.5			9828.442	-1			7797.275	-4	9776.505	-2	9766.173	-4
22.5			9827.760	8			7796.724	14	9776.296	10	9765.493	6
23.5	9838.361	1	9827.042	1			7796.129	4	9776.046	1	9764.773	-4
24.5	9838.098	-1	9826.312	2	7807.305	-12	7795.525	-1	9775.783	-0	9764.054	8
25.5	9837.820	1	9825.553	-5	7807.174	0	7794.909	-4	9775.498	-3	9763.300	4
26.5	9837.519	1	9824.785	-1	7807.015	-1	7794.287	3	9775.206	7	9762.521	-4
27.5	9837.203	6	9823.995	2	7806.844	1	7793.638	-2	9774.866	-11	9761.734	1
28.5	9836.851	-4	9823.182	0	7806.657	2	7792.980	-2	9774.528	-6	9760.921	-2
29.5	9836.496	2	9822.346	-3	7806.455	3	7792.305	-2				
30.5	9836.112	0	9821.496	-1	7806.240	5	7791:619	-0	9773.782	-5	9759.242	4
31.5	9835.706	-4	9820.621	-2	7806.004	2	7790.916		9773.388	4	9758.366	-1
32.5	9835.283	-4	9819.727	-3	7805.754	-1	7790.193	-5	9772.961	1	9757.483	9
33.5	9834.850	7	9818.819	2	7805.494	2	7789.474	8			9756.564	2
34.5	9834.374	-6	9817.886	4	7805.217	2	7788.720	2	9772.044	-7	9755.627	-2
35.5	9833.896	-1	9816.925	-4	7804.916	-7	7787.957	1	9771.564	-2	9754.679	3
36.5	9833.395	3			7804.617	2			9771.058	-3	9753.703	1
37.5	9832.868	0	9814.958	-2	7804.294	0	7786.392	6	9770.538	3	9752.711	2
38.5	9832.325	2	9813.948	2	7803.961	4	7785.579	0	9769.992	4	9751.697	2
39.5	9831.761	3	9812.909	-1	7803.604	0	7784.758	1	9769.426	4	9750.662	2
40.5	9831.167	-5			7803.238	0	7783.911	-9	9768.839	4	9749.606	-0
41.5	9830.564	-2	9810.782	2	7802.862	7	7783.070	2	9768.225	-3	9748.532	0
42.5	9829.942	2	9809.680	-4	7802.460	2	7782.204	2	9767.603	2	9747.438	1
43.5	9829.298	4	9808.571	3	7802.050	4	7781.322	2	9766.954	1	9746.319	-3
44.5	9828.628	1	9807.434	3	7801.622	3	7780.418	-6	9766.281	-4	9745.185	-1
45.5	9827.938	-1	9806.278	3	7801.180	3	7779.514	1	9765.596	0	9744.035	5
46.5	9827.229	-2	9805.099	1	7800.720	1			9764.888	1	9742.857	3
47.5	9826.502	-2	9803.895	-5	7800.248	0	7777.643	-2	9764.157	-0	9741.660	2
48.5	9825.758	3	9802.685	1	7799.762	2	7776.687	-2	9763.410	2	9740.440	-2
49.5	9824.983	-2	9801.438	-7	7799.265	7	7775.720	1	9762.647	10	9739.205	0
50.5	9824.194	-2	9800.185	-3	7798.741	-0			9761.849	2	9737.951	3
51.5	9823.385	-2			7798.209	0	7773.730	-2	9761.033	-3	9736.671	1
52.5	9822.565	9	9797.611	1	7797.662	0	7772.714	-2			9735.374	1
53.5	9821.706	0	9796.292	-0	7797.095	-4	7771.688	3	9759.351	-1	9734.057	2
54.5	9820.834	-0	9794.951	-1	7796.510	-11	7770.638	-2	9758.475	-5	9732.712	-4
55.5	9819.944	1	9793.594	1	7795.930	1	7769.584	4	9757.584	-2	9731.353	-4

TABLE 1—*Continued*

J	R(J)	Δν	P(J)	Δν	R(J)	Δν	P(J)	Δν	R(J)	Δν	P(J)	Δν
56.5	9819.028	-2	9792.210	-3	7795.321	-0	7768.503	-1	9756.671	-2	9729.985	7
57.5	9818.095	-3			7794.701	2	7767.412	-2	9755.740	1	9728.584	5
58.5	9817.144	-1			7794.062	1	7766.307	-2	9754.789	3	9727.167	7
59.5			9787.954	2	7793.410	2	7765.184	-4	9753.812	1	9725.720	0
60.5	9815.178	1	9786.487	-4	7792.730	-10	7764.057	4	9752.819	4	9724.258	-2
61.5	9814.163	1	9785.012	3	7792.061	5	7762.899	-3	9751.798	-2	9722.782	3
62.5	9813.130	3	9783.509	2	7791.356	-2	7761.726	-11	9750.765	2	9721.276	-2
63.5	9812.070	-2	9781.983	-1	7790.645	1	7760.559	2	9749.709	3	9719.762	5
64.5	9810.999	3	9780.438	-4	7789.914	-1	7759.361	-0	9748.631	2	9718.218	3
65.5	9809.900	1	9778.882	3	7789.173	2	7758.154	2	9747.529	-2	9716.652	-2
66.5	9808.784	2	9777.296	-0	7788.420	8	7756.920	-6	9746.419	6	9715.068	-3
67.5	9807.645	0	9775.693	0	7787.622	-16	7755.682	-4	9745.273	-1	9713.468	-1
68.5	9806.488	2	9774.074	6	7786.837	-11	7754.421	-9	9744.113	-2	9711.848	2
69.5			9772.425	1	7786.036	-7	7753.157	-3	9742.929	-6	9710.196	-6
70.5	9804.110	2	9770.756	-3	7785.222	-2	7751.880	5	9741.732	-2	9708.535	-3
71.5	9802.886	-1	9769.075	2	7784.386	-2	7750.574	-1	9740.511	-2	9706.852	-2
72.5			9767.366	-2	7783.539	0	7749.249	-10	9739.269	-3	9705.151	1
73.5	9800.391	5	9765.639	-3	7782.669	-4	7747.934	6	9738.010	0	9703.421	-4
74.5	9799.107	3	9763.895	-0	7781.785	-7	7746.556	-27	9736.729	3	9701.678	-1
75.5	9797.804	2					7745.213	-9	9735.426	3		
76.5	9796.482	3			7779.986	2	7743.851	5	9734.096	-3		
77.5	9795.134	-1	9758.527	-7	7779.058	1	7742.443	-12	9732.749	-6		
78.5	9793.770	-1	9756.705	-0			7741.049	-1	9731.390	1		
79.5			9754.859	3	7777.163	5						
80.5			9752.983	-4	7776.183	-2	7738.195	3				
81.5	9789.550	-4	9751.097	-1	7775.194	-3	7736.750	10				
82.5	9788.105	-2	9749.190	1	7774.190	-4	7735.278	4				
83.5	9786.643	3	9747.258	1	7773.166	-8	7733.799	7				
84.5	9785.157	6	9745.311	4	7772.141	0	7732.298	2				
85.5	9783.642	-0	9743.334	-2	7771.084	-7	7730.779	-5				
86.5	9782.112	-0	9741.342	-1	7770.028	2	7729.252	-5				
87.5	9780.565	3	9739.330	-1					9718.170	-2		
88.5			9737.298	0	7767.855	5			9716.603	3		
89.5	9777.395	-3	9735.240	-4	7766.750	11			9715.001	-6		
90.5	9775.783	-3	9733.171	1	7765.623	11			9713.393	-1		
91.5			9731.073	-3					9711.755	-4		
92.5			9728.963	2					9710.109	5		
93.5	9770.822	-1	9726.825	0					9708.428	-1		
94.5	9769.125	-2	9724.668	-1					9706.730	-2		
95.5	9767.411	1	9722.491	-1								
96.5			9720.292	-2					9703.283	7		
97.5			9718.079	3					9701.521	3		
98.5			9715.844	6								
99.5			9713.580	2								
100.5			9711.301	2								
101.5	9756.671	-1	9708.999	1								
102.5			9706.675	-3								
103.5	9752.914	-11	9704.337	1								
104.5	9751.012	-9	9701.978	5								
105.5	9749.092	-3										
106.5	9747.153	5										
107.5	9745.185	4										
108.5	9743.192	-1										
109.5	9741.182	-2										
110.5	9739.154	2										
111.5	9737.103	2										
112.5	9735.026	-3										
113.5	9732.929	-7										
114.5	9730.830	9										
115.5	9728.684	-1										
116.5	9726.518	-11										
117.5	9724.348	-3										
118.5	9722.149	-3										
119.5	9719.926	-6										
120.5	9717.694	3										
121.5	9715.432	4										
122.5	9713.150	5										
123.5	9710.842	1										

TABLE 1—*Continued*

J	R(J)	Δν	P(J)	Δν	R(J)	Δν	P(J)	Δν	R(J)	Δν	P(J)	Δν	R(J)	Δν	P(J)	Δν
	$[9.4]^2\Phi_{5/2}$ - $a^2\Phi_{5/2}$ 0-3				$[9.4]^2\Phi_{5/2}$ - $a^2\Phi_{5/2}$ 1-2				$[9.4]^2\Phi_{5/2}$ - $a^2\Phi_{5/2}$ 1-3				$[9.4]^2\Phi_{5/2}$ - $a^2\Phi_{5/2}$ 1-4			
11.5							9133.987	8								
12.5							9133.534	6								
13.5							9133.067	8								
14.5					9139.677	6	9132.580	6								
15.5			8369.833	-31	9139.634	-7	9132.061	-10								
16.5			8369.384	-16	9139.596	2	9131.559	8							8316.996	-13
17.5			8368.905	-18	9139.527	-2	9131.010	-3							8316.517	-7
18.5			8368.423	-8	9139.441	-7	9130.460	1								
19.5							9129.890	2							8315.500	-9
20.5					9139.231	-2	9129.294	-5								
21.5					9139.093	-6	9128.689	-4							8314.438	-0
22.5					9138.943	-6	9128.073	3							8313.877	-4
23.5			8365.758	-6	9138.788	7	9127.445	15	8729.338	-11			8324.662	1	8313.313	4
24.5	8377.060	-7	8365.197	9	9138.596	-0	9126.764	-8	8729.208	-13			8324.539	-9	8312.719	-5
25.5	8376.952	0	8364.596	-3	9138.407	12	9126.093	-4	8729.071	-6			8324.417	-4	8312.118	-5
26.5	8376.816	-6	8363.994	-1	9138.174	-1	9125.407	1	8728.899	-18	8716.144	-5	8324.257	-21	8311.511	2
27.5	8376.676	-3			9137.932	-6	9124.699	3	8728.737	-6	8715.493	-9	8324.128	6	8310.876	-3
28.5	8376.517	-3	8362.751	7	9137.683	-1	9123.975	5	8728.552	-1	8714.841	1	8323.942	-9	8310.234	-3
29.5	8376.347	-1			9137.401	-11	9123.228	1	8728.346	-1	8714.159	-3	8323.769	4	8309.589	10
30.5	8376.159	-1	8361.435	-0	9137.121	-3	9122.463	-4	8728.131	5	8713.469	0	8323.568	3		
31.5	8375.956	-3	8360.756	-4	9136.805	-13	9121.691	2	8727.891	2	8712.764	4	8323.351	1		
32.5	8375.749	6	8360.069	-0	9136.497	2	9120.896	2	8727.639	1	8712.025	-11	8323.123	3		
33.5	8375.513	1			9136.156	1	9120.074	-7	8727.368	-2			8322.882	5		
34.5	8375.272	5	8358.648	2	9135.802	4	9119.255	3	8727.081	-4	8710.539	-1	8322.619	0		
35.5	8375.012	5	8357.907	-6	9135.419	-3	9118.402	-3	8726.792	6	8709.774	4	8322.347	2	8305.327	-2
36.5	8374.741	9	8357.164	-0	9135.036	6	9117.540	-2	8726.477	5	8708.989	7	8322.056	-2	8304.567	-3
37.5	8374.443	0	8356.406	5	9134.635	14	9116.665	4	8726.151	11	8708.175	-6	8321.767	11	8303.803	6
38.5	8374.144	6	8355.627	4	9134.192	-2	9115.769	6			8707.365	3	8321.446	7	8303.005	-3
39.5	8373.825	6	8354.828	-3	9133.753	3			8725.432	2	8706.531	4	8321.115	7	8302.208	3
40.5	8373.484	-1	8354.025	2	9133.293	4	9113.916	0	8725.058	7	8705.668	-9	8320.767	6	8301.395	7
41.5			8353.203	2	9132.806	-5	9112.966	1	8724.662	6	8704.814	3	8320.406	5	8300.558	3
42.5	8372.780	8	8352.367	3	9132.316	2	9111.998	-1	8724.244	-1	8703.953	24			8299.715	6
43.5	8372.392	-1			9131.806	5	9111.014	-0	8723.824	6	8703.038	7	8319.642	7	8298.854	6
44.5	8371.996	-2	8350.651	7	9131.267	-3	9110.008	-6	8723.387	13	8702.119	2	8319.238	8	8297.972	-0
45.5	8371.591	2	8349.768	6			9108.996	1	8722.916	2	8701.187	0	8318.807	-2	8297.079	-3
46.5			8348.861	-3	9130.157	0	9107.939	-20			8700.239	-1	8318.370	-4	8296.175	-1
47.5	8370.715	-8	8347.958	6	9129.575	1	9106.902	-5			8699.278	1	8317.924	-0	8295.261	5
48.5	8370.268	-1	8347.018	-6	9128.977	2	9105.838	1			8698.298	0			8294.319	-2
49.5	8369.791	-7	8346.082	2	9128.358	0	9104.743	-6			8697.296	-6			8293.372	1
50.5	8369.308	-4	8345.123	1	9127.723	0	9103.648	4	8720.372	3	8696.284	-6	8316.479	-6	8292.403	-4
51.5	8368.823	14	8344.154	5	9127.070	-1	9102.531	8	8719.817	7	8695.262	-0			8291.428	1
52.5	8368.304	11	8343.160	0	9126.404	2	9101.381	-2	8719.233	-3	8694.213	-5	8315.445	-6	8290.435	2
53.5			8342.155	-0	9125.714	-1	9100.220	-8	8718.643	-2	8693.156	-1			8289.423	-0
54.5			8341.128	-7	9125.007	-4	9099.072	18	8718.033	-3	8692.071	-8	8314.356	-0	8288.382	-18
55.5			8340.100	-1	9124.291	1	9097.866	2			8690.971	-13	8313.787	1	8287.359	-1
56.5			8339.040	-10	9123.546	-5	9096.649	-7	8716.766	-4	8689.863	-11	8313.196	-6	8286.301	-5
57.5	8365.478	4	8337.985	1	9122.790	-4			8716.099	-12	8688.742	-5			8285.232	-5
58.5	8364.876	13	8336.902	-0			9094.205	18	8715.442	6	8687.596	-7	8311.992	7	8284.148	-4
59.5	8364.237	0	8335.796	-9	9121.229	-1	9092.934	6	8714.743	-1	8686.439	-4	8311.354	-1	8283.064	11
60.5	8363.594	-1	8334.690	-2			9091.673	22	8714.029	-7	8685.260	-5	8310.711	2	8281.939	-0
61.5	8362.920	-17	8333.553	-11	9119.595	-1	9090.348	-9	8713.292	-19	8684.057	-15	8310.032	-16	8280.806	-3
62.5	8362.271	8	8332.419	-1	9118.757	5	9089.049	4	8712.543	-25	8682.863	2	8309.357	-15	8279.662	-3
63.5			8331.255	-6	9117.893	1	9087.718	2	8711.803	-7	8681.630	-4			8278.499	-6
64.5	8360.874	5	8330.080	-5	9117.012	-2	9086.388	17	8711.029	-5	8680.386	-5			8277.330	1
65.5	8360.150	2	8328.886	-8			9085.009	1	8710.241	0	8679.133	3			8276.136	-3
66.5	8359.418	6			9115.212	7	9083.626	-1	8709.422	-9	8677.851	-2			8274.933	0
67.5					9114.275	-0	9082.230	1			8676.558	-1			8273.710	-1
68.5					9113.327	-0	9080.813	-1	8707.764	3	8675.255	6	8305.003	15	8272.475	-0
69.5	8357.108	1			9112.356	-6	9079.380	-2	8706.893	-8	8673.922	-0	8304.204	1	8271.220	-3
70.5	8356.310	2			9111.383	4			8706.023	-2	8672.581	3	8303.404	2	8269.955	-1
71.5	8355.500	8			9110.386	7	9076.463	-2	8705.125	-5	8671.221	3	8302.600	14	8268.690	18
72.5	8354.664	2	8320.124	0	9109.359	-2	9074.980	-1			8669.845	5	8301.758	5	8267.376	2
73.5	8353.820	5	8318.807	-2	9108.326	0	9073.482	2	8703.294	0	8668.451	3	8300.918	12		
74.5			8317.476	-2	9107.273	-0	9071.958	-3	8702.353	4	8667.044	6				

TABLE 1—*Continued*

J	R(J)	Δν	P(J)	Δν	R(J)	Δν	P(J)	Δν	R(J)	Δν	P(J)	Δν	R(J)	Δν	P(J)	Δν
75.5			8316.123	-10	9106.204	1	9070.424	-1	8701.406	17	8665.614	3				
76.5			8314.763	-9	9105.106	-9	9068.874	2	8700.415	3	8664.174	5				
77.5					9104.006	-4	9067.300	-1	8699.418	-1	8662.719	10				
78.5					9102.878	-9	9065.709	-3	8698.421	13	8661.248	14				
79.5					9101.749	2	9064.109	2			8659.746	3				
80.5							9062.480	-4			8658.243	8				
81.5					9099.412	-1	9060.846	2			8656.723	11				
82.5					9098.216	-4	9059.186	-1								
83.5					9097.011	1	9057.507	-5			8653.614	-3				
84.5					9095.781	-1	9055.822	2			8652.047	1				
85.5					9094.531	-5	9054.106	-4			8650.447	-12				
86.5					9093.272	-0	9052.382	-2			8648.846	-11				
87.5					9091.994	2	9050.639	-0			8647.228	-11				
88.5					9090.693	-0	9048.874	-3								
89.5					9089.380	3	9047.102	3								
90.5					9088.048	5	9045.304	2								
91.5					9086.688	-4	9043.491	2								
92.5							9041.658	1								
93.5					9083.943	6	9039.808	-0								
94.5					9082.534	2	9037.934	-8								
95.5					9081.109	-1	9036.057	-2								
96.5					9079.672	1	9034.160	2								
97.5					9078.224	11	9032.236	-4								
98.5					9076.736	-2	9030.305	1								
99.5					9075.232	-13	9028.354	2								
100.5					9073.734	-1	9026.382	2								
101.5					9072.211	4										
102.5					9070.667	6	9022.385	-2								
103.5					9069.096	-1	9020.357	-7								
104.5					9067.515	-1	9018.327	4								
105.5					9065.925	8	9016.269	3								
106.5					9064.306	6	9014.184	-6								
107.5					9062.662	-3										
108.5					9061.019	6										
109.5					9059.345	3										
110.5					9057.650	-5										
111.5					9055.948	-1										
112.5					9054.222	-3										
113.5					9052.482	-2										
114.5					9050.730	6										

7714 cm^{-1} are the 0–1, 0–0, and 1–0 bands of another new subband with the $a^2\Phi_{5/2}$ spin component as its lower state. These bands are much weaker in intensity than the bands described previously. A compressed portion of the spectrum showing the 0–1 bands of the two subbands is provided in Fig. 3. The present observation suggests that the excited state of this transition is either a $^2\Delta$ or a $^2\Gamma$ state. It is difficult to decide between the $^2\Delta$ or the $^2\Gamma$ assignment because the intensity of the *R* and *P* branches is similar and the *Q* branch is most intense. No Ω doubling has been observed in any of the bands. In the present paper we have preferred the $^2\Delta$ assignment on the basis of the theoretical predictions of Focsa *et al.* for TiCl (*13*) and ZrCl (*14*).

The rotational assignments in the different bands were made by comparing combination differences for the common vibrational levels. The observed electronic states probably belong to Hund's case (a) coupling but the subbands were not fitted together. Rather than fitting all of the lines together with assumed spin–orbit constants, we decided to use the following simple empirical term energy expression for each spin component:

$$F_v(J) = T_v + B_vJ(J+1) - D_v[J(J+1)]^2 + H_v[(J+1)]^3. \quad [1]$$

Initially a band-by-band fit was obtained for each subband. This fit provided similar constants for common vibrational levels, confirming the vibrational assignments. In the final fit, the lines of all of the vibrational bands of each subband with a common lower state were combined and fitted simultaneously. The observed line positions for the new bands of the $[9.4]^2\Phi$–$a^2\Phi$ transition are provided in Table 1 while the line positions for the new $[7.3]^2\Delta$–$a^2\Phi$ transition are provided in Table 2. The rotational constants were determined by weighting the individual lines according to signal-to-noise ratio and extent of blending. Badly blended lines were heavily deweighted. The

TABLE 2
Observed Line Positions (in cm^{-1}) for the $[7.3]^2\Delta$–$a^2\Phi$ System of ZrCl

J	R(J)	Δν	Q(J)	Δν	P(J)	Δν	R(J)	Δν	Q(J)	Δν	P(J)	Δν
	$[7.3]^2\Delta_{5/2}$ - $a^2\Phi_{7/2}$ 0-0						$[7.3]^2\Delta_{5/2}$ - $a^2\Phi_{7/2}$ 0-1					
8.5			7245.372	-8					6833.999	4		
9.5			7245.218	3					6833.844	4		
10.5									6833.657	-11		
11.5			7244.834	2					6833.486	6		
12.5			7244.606	-8					6833.272	-4		
13.5			7244.383	3					6833.051	-5		
14.5									6832.815	-4		
15.5									6832.567	1		
16.5			7243.562	-8					6832.294	-2		
17.5									6832.014	4		
18.5			7242.944	1					6831.701	-7		
19.5			7242.608	4					6831.383	-6		
20.5	7247.380	1	7242.253	6	7237.356	1			6831.055	0		
21.5	7247.242	-1	7241.866	-7	7236.743	2	6836.073	-0	6830.698	-5		
22.5			7241.484	3	7236.116	4	6835.939	-4	6830.331	-5		
23.5	7246.918	-1	7241.074	2	7235.477	13	6835.808	10	6829.951	0		
24.5			7240.650	5	7234.798	-1	6835.627	-9	6829.555	4		
25.5	7246.520	-4	7240.205	4	7234.113	-3	6835.463	6	6829.135	0		
26.5			7239.740	0	7233.427	11	6835.253	-9	6828.694	-7		
27.5			7239.267	6			6835.060	9	6828.246	-5		
28.5			7238.767	3	7231.966	1	6834.822	-2	6827.783	-3		
29.5	7245.531	4	7238.252	1	7231.204	-9	6834.567	-13	6827.298	-5		
30.5	7245.218	-16	7237.723	3	7230.438	-6	6834.318	-1	6826.809	4		
31.5	7244.923	-1	7237.164	-7			6834.042	-0	6826.290	0		
32.5	7244.606	11	7236.599	-6	7228.836	-16	6833.745	-4	6825.756	-2		
33.5	7244.252	3	7236.026	6	7228.031	1	6833.437	-2	6825.215	4		
34.5	7243.886	0	7235.431	11	7227.188	-3	6833.102	-10	6824.645	-1		
35.5	7243.508	3	7234.798	-3	7226.324	-11	6832.770	-0	6824.062	-4		
36.5	7243.101	-6	7234.158	-7			6832.412	2	6823.479	10		
37.5	7242.693	2	7233.509	-2					6822.854	-1		
38.5	7242.253	-5							6822.230	5		
39.5	7241.812	6	7232.163	11	7222.730	-4	6831.233	-1	6821.579	0		
40.5	7241.334	-5	7231.446	0	7221.783	-7	6830.808	-1	6820.916	-0		
41.5	7240.853	1	7230.724	3			6830.367	-1	6820.249	12		
42.5			7229.997	17					6819.542	1		
43.5			7229.220	-2					6818.828	-0		
44.5			7228.447	1			6828.942	-1	6818.098	-2		
45.5			7227.649	-3			6828.441	5	6817.356	0		
46.5	7238.161	2					6827.916	4	6816.592	-2		
47.5	7237.568	1					6827.367	-4	6815.818	2		
48.5	7236.959	2	7225.161	-4			6826.809	-5	6815.027	6		
49.5			7224.302	0			6826.240	0	6814.208	-3		
50.5	7235.677	-9	7223.423	3			6825.651	1	6813.386	3		
51.5	7235.030	5	7222.516	-5			6825.047	4	6812.536	-3		
52.5	7234.345	0	7221.594	-10					6811.681	2		
53.5			7220.670	-0			6823.768	-11	6810.799	-3		
54.5			7219.709	-9			6823.120	-2	6809.912	3		
55.5	7232.204	5	7218.746	-3			6822.455	5	6808.999	0		
56.5	7231.446	-3	7217.763	2			6821.764	5	6808.070	-3		
57.5	7230.681	0	7216.752	-5			6821.043	-10	6807.128	-2		
58.5	7229.883	-12	7215.733	-2			6820.333	3	6806.170	0		
59.5	7229.078	-13	7214.695	1			6819.595	4	6805.211	17		
60.5			7213.640	2			6818.828	-6	6804.203	1		
61.5			7212.563	1					6803.194	1		
62.5			7211.457	-12					6802.167	-0		
63.5			7210.363	4					6801.127	3		
64.5			7209.232	2					6800.066	0		
65.5			7208.091	6					6798.993	3		
66.5												
67.5			7205.729	-10								
68.5			7204.540	-1								
69.5			7203.320	-4								

Note. $\Delta\nu$'s are observed minus calculated wavenumbers in the units of 10^{-3} cm^{-1}.

TABLE 2—*Continued*

J	R(J)	Δν	Q(J)	Δν	P(J)	Δν	R(J)	Δν	Q(J)	Δν	P(J))	Δν
			$[7.3]^2\Delta_{3/2}$ - $a^2\Phi_{5/2}$ 0-1						$[7.3]^2\Delta_{3/2}$ - $a^2\Phi_{5/2}$ 0-0			
6.5			6939.471	-2								
7.5									7350.600	-11		
8.5			6939.187	2					7350.440	-9		
9.5			6939.014	0					7350.270	3		
10.5			6938.823	-2					7350.071	4		
11.5			6938.617	-1					7349.855	7		
12.5			6938.391	-2					7349.601	-8		
13.5			6938.152	3	6934.966	14			7349.353	2		
14.5									7349.074	-1		
15.5	6941.508	-10	6937.613	3	6933.944	6			7348.767	-13	7345.106	-2
16.5	6941.449	-9	6937.310	-3	6933.397	-8			7348.466	1	7344.553	-3
17.5	6941.378	-1	6936.994	-3	6932.858	5			7348.136	5	7343.994	8
18.5			6936.662	-2	6932.285	2	7352.396	0	7347.781	3	7343.401	4
19.5	6941.175	7	6936.316	2			7352.274	13	7347.408	2	7342.792	5
20.5	6941.037	1	6935.939	-6	6931.090	0	7352.115	9				
21.5			6935.562	5					7346.608	4	7341.506	-7
22.5	6940.715	-2	6935.149	-3	6929.824	1	7351.747	7	7346.170	-5	7340.839	-9
23.5	6940.529	-1	6934.726	-3	6929.174	10	7351.517	-11	7345.733	6		
24.5	6940.329	4	6934.290	2	6928.488	2	7351.302	5	7345.264	5	7339.457	-1
25.5	6940.105	3	6933.826	-3	6927.791	0	7351.045	-2	7344.778	5	7338.732	-3
26.5	6939.860	-2	6933.352	1	6927.078	1	7350.772	-6	7344.268	0	7337.993	-1
27.5	6939.610	6	6932.858	2	6926.344	-2	7350.489	-1	7343.741	-2	7337.226	-6
28.5			6932.343	0	6925.598	3	7350.183	0	7343.193	-6	7336.450	-2
29.5			6931.811	-0	6924.836	8	7349.855	-1	7342.633	-4	7335.650	-2
30.5	6938.719	0	6931.260	-3	6924.036	-6			7342.055	1	7334.828	-7
31.5	6938.391	3	6930.691	-4			7349.152	6	7341.457	3	7333.991	-6
32.5	6938.042	3	6930.110	-0	6922.410	-7	7348.767	5	7340.839	6	7333.137	-4
33.5	6937.669	-3	6929.504	-2	6921.581	4	7348.360	1			7332.275	9
34.5			6928.888	3	6920.714	-7	7347.925	-12	7339.534	-2	7331.367	-3
35.5	6936.889	6	6928.237	-9			7347.498	2	7338.855	-3	7330.456	-1
36.5			6927.590	2	6918.946	-6			7338.160	-2		
37.5	6936.022	-0	6926.915	2			7346.559	3	7337.445	-1		
38.5	6935.562	-3	6926.223	3	6917.114	3	7346.060	3	7336.711	-0	7327.591	-11
39.5	6935.097	7	6925.506	-3	6916.161	-3	7345.535	-5	7335.959	1		
40.5	6934.591	-6	6924.784	5	6915.199	1	7345.005	3	7335.183	-3	7325.595	-9
41.5	6934.091	6	6924.036	5	6914.220	6	7344.442	-4	7334.396	3	7324.575	-1
42.5	6933.555	0	6923.263	-3	6913.217	3	7343.868	-3	7333.582	-0	7323.528	-1
43.5	6933.017	10	6922.483	0	6912.193	-1	7343.268	-8	7332.752	-0	7322.470	7
44.5	6932.430	-12	6921.678	-3					7331.903	-0	7321.386	8
45.5	6931.859	2	6920.867	5					7331.033	-2	7320.274	-1
46.5	6931.260	4	6920.020	-4	6909.025	-4	7341.375	-4	7330.146	-1		
47.5	6930.638	2	6919.172	3	6907.935	-3	7340.708	0	7329.241	1		
48.5	6929.990	-8			6906.822	-7	7340.017	-0	7328.315	-0		
49.5			6917.400	-4	6905.701	-0	7339.309	1	7327.367	-4		
50.5	6928.668	1	6916.498	4	6904.561	4	7338.568	-11	7326.407	1	7314.473	4
51.5	6927.973	-1	6915.568	2	6903.402	9	7337.826	-6	7325.424	1	7313.250	-1
52.5	6927.254	-10	6914.619	-2	6902.211	-2	7337.062	-3	7324.424	3	7312.014	0
53.5	6926.537	1	6913.666	9	6901.009	-5	7336.281	2	7323.398	-2	7310.758	1
54.5	6925.782	-7	6912.672	-4	6899.796	-1	7335.473	-1	7322.361	1	7309.487	6
55.5	6925.026	2	6911.674	-2	6898.552	-10	7334.649	-0	7321.301	0	7308.189	2
56.5	6924.242	0	6910.657	-0	6897.310	1	7333.806	1	7320.221	-1		
57.5	6923.449	8	6909.622	0	6896.042	4	7332.939	-4	7319.126	2		
58.5	6922.624	2	6908.566	-2	6894.756	6	7332.057	-4	7318.009	1	7304.185	-4
59.5	6921.786	1	6907.497	1	6893.439	-4	7331.157	-4	7316.863	-9		
60.5	6920.928	-1	6906.410	4	6892.106	-12	7330.243	3	7315.719	1	7301.432	3
61.5	6920.060	4	6905.294	-4	6890.772	-4	7329.294	-6	7314.541	-2	7300.018	-3
62.5	6919.172	8	6904.173	1	6889.423	8			7313.351	1		
63.5			6903.030	1	6888.035	-1			7312.134	-4		
64.5	6917.322	-5	6901.868	1	6886.639	-1	7326.360	-7	7310.909	2		
65.5	6916.382	1	6900.684	-2	6885.220	-5	7325.347	-3	7309.658	2	7294.195	-1
66.5	6915.417	-0	6899.487	-1			7324.315	0	7308.385	-1	7292.693	2
67.5	6914.430	-5	6898.277	6	6882.353	10			7307.093	-4	7291.163	-5
68.5	6913.429	-6	6897.040	2	6880.878	3	7322.187	1	7305.791	1	7289.632	6
69.5	6912.427	11			6879.396	8			7304.465	2		
70.5	6911.382	2	6894.514	-1					7303.118	2	7286.476	-9

TABLE 2—*Continued*

J	R(J)	Δν	Q(J)	Δν	P(J)	Δν	R(J)	Δν	Q(J)	Δν	P(J))	Δν
71.5	6910.325	0	6893.227	1			7318.852	3	7301.748	-2	7284.883	-3
72.5	6909.252	-0	6891.918	-2			7317.697	-2	7300.366	0		
73.5	6908.167	5	6890.595	-0					7298.962	-1	7281.633	3
74.5	6907.052	-1	6889.258	6			7315.337	-3	7297.543	3	7279.976	2
75.5	6905.933	7	6887.894	1			7314.133	2	7296.097	-1	7278.302	3
76.5			6886.509	-5			7312.898	-5	7294.642	5		
77.5			6885.120	2			7311.651	-6			7274.885	-6
78.5			6883.705	2			7310.399	8	7291.656	-2	7273.161	3
79.5			6882.266	-4			7309.111	6	7290.140	0	7271.411	4
80.5			6880.820	1			7307.810	10	7288.599	-3	7269.630	-6
81.5			6879.343	-7			7306.475	-2	7287.042	-3		
82.5			6877.871	8			7305.150	17	7285.461	-8	7266.035	-3
83.5			6876.359	1			7303.772	1	7283.878	4	7264.209	-1
84.5							7302.389	-0	7282.262	2		
85.5									7280.634	7		
86.5									7278.972	-3		
87.5									7277.303	-0		
88.5									7275.605	-7		
89.5									7273.908	6		
90.5									7272.176	3		
91.5									7270.415	-9		
92.5									7268.654	-3		
93.5									7266.868	-3		
94.5									7265.058	-6		

J	R(J)	Δν	Q(J)	Δν	P(J)	Δν	J	R(J)	Δν	Q(J)	Δν	P(J)	Δν
							[7.3]$^2\Delta_{3/2}$ - $a^2\Phi_{5/2}$ 1-0						
9.5			7712.857	-7			44.5	7704.225	-16	7693.524	-3	7683.048	1
10.5			7712.658	4	7710.185	8	45.5	7703.576	15	7692.615	3	7681.903	5
11.5			7712.422	0	7709.711	1	46.5			7691.678	-0	7680.743	14
12.5			7712.168	-3	7709.225	2	47.5			7690.723	-0	7679.544	4
13.5			7711.904	4	7708.708	-8	48.5	7701.394	-7	7689.748	-1	7678.319	-12
14.5			7711.609	1			49.5	7700.632	-9	7688.754	0		
15.5			7711.296	-1	7707.636	-6	50.5	7699.860	-0	7687.746	6	7675.854	2
16.5	7715.092	-0	7710.961	-5	7707.089	14	51.5	7699.060	-0	7686.705	0	7674.583	-1
17.5	7714.972	-5	7710.617	2	7706.491	3	52.5	7698.237	-2	7685.651	2	7673.289	-5
18.5	7714.840	-1	7710.236	-7			53.5	7697.407	9	7684.579	4	7671.986	2
19.5	7714.673	-12	7709.859	8	7705.243	-10	54.5	7696.534	-3	7683.474	-5	7670.658	3
20.5	7714.514	5	7709.443	4	7704.618	13	55.5	7695.654	-1	7682.366	2	7669.305	-1
21.5	7714.313	1	7708.994	-13	7703.928	-9	56.5	7694.753	-1	7681.221	-8	7667.935	-2
22.5	7714.097	1	7708.557	2	7703.251	1	57.5	7693.828	-4	7680.077	4	7666.539	-8
23.5	7713.862	2	7708.075	-8			58.5	7692.888	-2	7678.903	6		
24.5	7713.603	0	7707.595	4	7701.824	10	59.5	7691.926	-3	7677.701	-0	7663.713	5
25.5	7713.332	6	7707.089	10	7701.060	-6	60.5			7676.487	1	7662.264	6
26.5	7713.033	4	7706.546	-0			61.5	7689.942	-2	7675.259	10	7660.787	-2
27.5	7712.707	-5	7705.997	4	7699.523	12	62.5			7673.994	0	7659.294	-5
28.5	7712.373	-2	7705.415	-6			63.5	7687.882	3	7672.724	6	7657.787	-2
29.5	7712.013	-5	7704.828	-1	7697.878	3	64.5	7686.832	17	7671.422	1	7656.259	-0
30.5			7704.225	9	7697.030	4	65.5	7685.738	5	7670.106	1		
31.5	7711.243	1	7703.576	-7	7696.147	-11	66.5	7684.627	-2	7668.771	3	7653.140	0
32.5	7710.826	1	7702.926	-3	7695.292	22	67.5			7667.418	7	7651.565	15
33.5	7710.383	-4			7694.367	5	68.5						
34.5	7709.924	-4	7701.565	2	7693.426	-8	69.5			7664.636	-1		
35.5	7709.443	-7	7700.854	3			70.5			7663.228	8		
36.5			7700.117	1	7691.502	-15	71.5	7678.806	-3	7661.784	1		
37.5	7708.438	4	7699.360	-4	7690.536	8	72.5			7660.317	-9		
38.5	7707.883	-12	7698.589	-1	7689.527	8	73.5			7658.842	-6		
39.5			7697.790	-6	7688.494	3	74.5	7675.078	4	7657.353	2		
40.5	7706.768	10	7696.983	0	7687.441	-2	75.5	7673.788	-1	7655.832	-1		
41.5	7706.144	-15	7696.147	-2	7686.379	6	76.5	7672.477	-6	7654.293	-2		
42.5	7705.540	1	7695.292	-3	7685.285	-0	77.5	7671.153	-4	7652.736	-1		
43.5	7704.898	-2	7694.418	-3	7684.174	-2	78.5			7651.164	6		

TABLE 3
Rotational Constants (in cm^{-1}) for the $a^2\Phi$, $[7.3]^2\Delta$, and $[9.4]^2\Phi$ States of ZrCl

State	Const.	v = 0	v = 1	v = 2	v = 3	v = 4	v = 5
$a^2\Phi_{7/2}$	T_v	a	a+411.42811(49)	a+818.6074(67)	a+1230.3311(30)	a+1631.96025(97)	a+2032.46924(85)
	B_v	0.12808311(99)	0.1275492(11)	0.126228(14)	0.1255980(39)	0.1258310(12)	0.1253840(11)
	$D_v \times 10^8$	4.9633(47)	5.0069(54)	-4.87(91)	-8.89(14)	4.333(10)	4.8833(82)
	$H_v \times 10^{10}$	--	--	-1.400(18)	-0.0893(15)	--	--
$a^2\Phi_{5/2}$	T_v	b	b+411.30660(31)	b+819.69619(34)	b+1229.8177(16)	b+1634.6648(14)	
	B_v	0.12799015(75)	0.12745472(76)	0.12690539(76)	0.1256645(19)	0.1254202(14)	
	$D_v \times 10^8$	4.9475(32)	4.9720(32)	5.0612(34)	-2.737(53)	3.114(20)	
	$H_v \times 10^{12}$	--	--	--	-3.852(47)	--	
$[7.3]^2\Delta_{5/2}$	T_v	a+7246.08242(77)					
	B_v	0.1193839(13)					
	$D_v \times 10^8$	5.524(19)					
$[7.3]^2\Delta_{3/2}$	T_v	b+7351.21882(44)	b+7713.86614(64)				
	B_v	0.11845211(80)	0.11794593(93)				
	$D_v \times 10^8$	5.0409(49)	5.0090(97)				
$[9.4]^2\Phi_{7/2}$	T_v	a+9133.29447(28)	a+9486.98964(31)	a+9838.40696(35)	a+10187.54793(82)		
	B_v	0.11904664(99)	0.11850779(99)	0.11796946(99)	0.1174321(11)		
	$D_v \times 10^8$	5.3858(47)	5.3907(48)	5.3944(47)	5.4051(68)		
$[9.4^2\Phi_{5/2}$	T_v	b+9605.11255(24)	b+9957.63173(23)	b+10307.86749(49)	b+10655.82833(61)		
	B_v	0.11885323(75)	0.11831283(76)	0.11777298(77)	0.11723364(78)		
	$D_v \times 10^8$	5.3862(32)	5.3901(32)	5.3927(34)	5.3957(36)		

Note. Values in parentheses are one standard deviation in the last digits and "a" and "b" refer to the undetermined term energies for the $a^2\Phi_{7/2}$ and $a^2\Phi_{5/2}$ spin components, respectively.

molecular constants for the $a^2\Phi$, $[7.3]^2\Delta$ and $[9.4]^2\Phi$ states are provided in Table 3.

RESULTS AND DISCUSSION

The constants of Table 3 clearly indicate the presence of interactions in the two spin components of the lower $a^2\Phi$ state. The molecular constants for the $v = 2$ and 3 vibrational levels of the $a^2\Phi_{7/2}$ and $a^2\Phi_{5/2}$ spin components indicate that these levels are affected by strong global interactions. Although no local perturbations have been observed in these vibrational levels, the vibrational intervals as well as the B_v and D_v constants have abnormal magnitudes. For example, the vibrational intervals of $\Delta G(1/2) = 411.42811(49)$ cm^{-1}, $\Delta G(3/2) = 407.1793(67)$ cm^{-1}, $\Delta G(5/2) = 411.7237(73)$ cm^{-1}, $\Delta G(7/2) = 401.6292(32)$ cm^{-1}, and $\Delta G(9/2) = 400.5090(13)$ cm^{-1} for the $a^2\Phi_{7/2}$ spin component and $\Delta G(1/2) = 411.30660(31)$ cm^{-1}, $\Delta G(3/2) = 408.38659(46)$ cm^{-1}, $\Delta G(5/2) = 410.1215(16)$, and $\Delta G(7/2) = 404.8471(21)$ cm^{-1} for the $a^2\Phi_{5/2}$ spin component have been observed. Similar irregular variations have been found for the rotational and distortion constants. Therefore, meaningful equilibrium molecular constants could not be determined for the $a^2\Phi$ state although approximate values of $\omega_e = 413.8952$ cm^{-1}, $\omega_e x_e = 1.2336$ cm^{-1}, $B_e = 0.12836$ cm^{-1}, and $\alpha_e = 0.00054$ cm^{-1} were estimated for the $a^2\Phi_{7/2}$ spin component by deweighting the values corresponding to the perturbed levels. The values of $\omega_e = 413.0669$ cm^{-1}, $\omega_e x_e = 0.8801$ cm^{-1}, $B_e = 0.12836$ cm^{-1}, and $\alpha_e = 0.00064$ cm^{-1} were estimated for the $a^2\Phi_{5/2}$ spin component in a similar manner. The constants for the $[7.3]^2\Delta_{3/2}$ spin component, for which $v = 0$ and 1 vibrational levels have been observed, have the values of $\Delta G(1/2) = 362.64732(78)$ cm^{-1}, $B_e = 0.1187052(10)$, and $\alpha_e = 0.0005062(12)$ cm^{-1}.

In contrast to the $a^2\Phi$ state, the constants for the $[9.4]^2\Phi$ state indicate that this state is free from perturbations. For example, the regular intervals of $\Delta G(1/2) = 353.69517(42)$ cm^{-1} $\Delta G(3/2) = 351.41732(47)$ cm^{-1} and $\Delta G(5/2) = 349.14097(89)$ cm^{-1} have been obtained for the $[9.4]^2\Phi_{7/2}$ spin component. This provides $\omega_e = 355.97225(70)$ cm^{-1}, and $\omega_e x_e = 1.13864(20)$ cm^{-1} for the $[9.4]^2\Phi_{7/2}$ spin component. The rotational constants for the different vibrational levels of the $[9.4]^2\Phi_{7/2}$ spin component are also very regular and provide the equilibrium constants of $B_e = 0.11931542(52)$ cm^{-1} and $\alpha_e = 0.00053822(24)$ cm^{-1}. The molecular constants for the $[9.4]^2\Phi_{5/2}$ spin component (Table 3) also do not show the influence of perturbations and provide the equilibrium constants of $\omega_e = 354.79904(30)\ \text{cm}^{-1}$, $\omega_e x_e = 1.14019(38)\ \text{cm}^{-1}$, $B_e = 0.11912290(38)\ \text{cm}^{-1}$, and $\alpha_e = 0.00053987(17)\ \text{cm}^{-1}$ for the $[9.4]^2\Phi_{5/2}$ spin component.

Prior to our very recent work on ZrCl (*5*), there were very limited spectroscopic studies. The initial studies of ZrCl had suggested a $^4\Sigma^-$ ground state for ZrCl (*1*, *2*), while our recent analysis of an infrared transition has suggested a $^4\Phi$ ground state (*5*) consistent with experimental observations for isovalent TiCl (*6*) and TiF (*7*). This observation has recently been supported by theoretical calculations of Focsa *et al.* for TiCl (*13*) and ZrCl (*14*). These calculations have also predicted the location of some states in the doublet manifold. In particular, they have predicted a $^2\Phi$ state located at 4810 cm^{-1} above the ground $X^4\Phi$ state is the first doublet excited state of ZrCl (*14*). The lower $a^2\Phi$ state observed in the present work is, therefore, the first excited doublet state of ZrCl. Three more low-lying doublet states $^2\Sigma^-$, $^2\Pi$, and $^2\Delta$ have been predicted at 6931 cm^{-1}, 7935 cm^{-1}, and 8886 cm^{-1} by the ligand field calculations of Focsa *et al.* (*14*). The $^2\Delta$ state observed in our spectrum near 7300 cm^{-1} can tentatively be assigned as the $^2\Delta$ state calculated by Focsa *et al.* (*14*) near 8886 cm^{-1} above the ground state. The location of the $[9.4]^2\Phi$ state has not been calculated by Fosca *et al.* (*14*) because it arises from a higher atomic configuration. High-quality *ab initio* calculations are necessary to confirm our assignments and the ligand field predictions. A reliable prediction of the spectroscopic properties of ZrCl will require the use of high-level *ab initio* calculations using large basis sets and an extensive treatment of electron correlation.

Our electronic assignments must be regarded as tentative since first lines were not measured. The most likely alternative assignments of $[7.3]^2\Phi$–$a^2\Delta$ and $[9.4]^2\Delta$–$a^2\Delta$ for our two electronic transitions cannot be ruled out yet.

We have noticed several small errors in the work of Phillips *et al.* (*4*). In particular the J assignment in the 1–3 band of the $[9.4]^2\Phi_{5/2}$–$a^2\Phi_{5/2}$ subband [their notation, $^2\Pi_{3/2}$-$^2\Pi_{3/2}$] needs to be increased by 2 units. It is worth mentioning that they stated in their paper that the *P* branch was not observed in the 1–3 band, while we have observed both *R* and *P* branches. We have also noticed that the *J* assignment in the 0–1, 0–0 and the 1–0 bands of the $[9.4]^2\Phi_{7/2}$–$a^2\Phi_{7/2}$ subband [their notation, $^2\Pi_{1/2}$–$^2\Pi_{1/2}$] needs to be increased by one unit, but this could be a misprint since the constants reported for this subband match very well with the values obtained in the present analysis.

CONCLUSIONS

The near infrared emission spectrum of ZrCl has been observed at high resolution using a Fourier transform spectrometer. Numerous new bands have been detected in the 6700–12 000 cm^{-1} region in addition to those reported previously by Phillips *et al.* (*4*). Six new bands observed near 9838, 9776, 8315, 8257, 7855, and 7806 cm^{-1} have been identified as 2–0, 3–1, 0–2, 1–3, 1–4 and 2–5 bands of the $[9.4]^2\Phi_{7/2}$–$a^2\Phi_{7/2}$ subband while additional new bands observed near 9137, 8727, 8375 and 8325 cm^{-1} have been identified as 1–2, 1–3, 0–3 and 1–4 bands of the $[9.4]^2\Phi_{5/2}$–$a^2\Phi_{5/2}$ subband. To lower wavenumbers, the bands found near 6835 and 7246 cm^{-1} have been assigned as the 0–1 and 0–0 bands of the $[7.3]^2\Delta_{5/2}$–$a^2\Phi_{7/2}$ subband and bands near 6940, 7351, and 7714 cm^{-1} have been assigned as the 0–1, 0–0, and 1–0 bands of the $[7.3]^2\Delta_{3/2}$–$a^2\Phi_{5/2}$ subband. Both of these transitions have the lower state in common. A rotational analysis of these bands has been obtained and molecular constants have been determined. The nature of the observed states has been discussed in light of the available theoretical results, but more calculations are needed.

ACKNOWLEDGMENTS

We thank J. Wagner and C. Plymate of the National Solar Observatory for assistance in obtaining the spectra. The National Solar Observatory is operated by the Association of Universities for Research in Astronomy, Inc., under contract with the National Science Foundation. The research described here was supported by funding from NASA laboratory astrophysics program. Some support was also provided by the Petroleum Research Fund administered by the American Chemical Society and the Natural Sciences and Engineering Research Council of Canada.

REFERENCES

1. P. K. Carroll and P. J. Daly, *Proc. Roy. Irish Acad.* **61**, 101–106 (1961).
2. K. J. Jordan, R. H. Lipson, N. A. McDonald, and D. S. Yang, *Chem. Phys. Lett*. **193**, 499–506 (1992).
3. T. Imajo, D. Wang, and K. Tanaka, Paper MG10, 54th International Symposium on Molecular Spectroscopy, Columbus, OH, June 1998.
4. J. G. Phillips, S. P. Davis and D. C. Galehouse, Astrophys. J. Suppl. Ser. **43**, 417–434 (1980).
5. R. S. Ram and P. F. Bernath, *J. Mol. Spectrosc*. **186**, 335–348 (1997).
6. R. S. Ram and P. F. Bernath, *J. Mol. Spectrosc*. **186**, 113–130 (1997).
7. R. S. Ram, J. R. D. Peers, Y. Teng, A. G. Adam, A. Muntianu, P. F. Bernath, and S. P. Davis, *J. Mol. Spectrosc*. **184**, 186–201 (1997).
8. J. F. Harrison, private communication
9. J. Anglada, P. J. Bruna and S. D. Peyerimhoff, *Mol. Phys*. **69**, 281–303 (1990).
10. T. C. Steimle, J. E. Shirley, B. Simard, M. Vasseur, and P. Hackett, *J. Chem. Phys*. **95**, 7179–7182 (1991).
11. O. Launila and B. Lindgren, *J. Chem. Phys*. **104**, 6418–6422 (1996).
12. A. Boldyrev and J. Simons, *J. Mol. Spectrosc*. **188**, 138–141 (1998).
13. C. Focsa, M. Bencheikh, and L. G. M. Pettersson, *J. Phys. B: At. Mol. Phys*. **31**, 2857- 2869 (1998).
14. C. Focsa, private communication.
15. R. S. Ram and P. F. Bernath, *J. Mol. Spectrosc.* **195,** 299–307 (1999).
16. R. B. LeBlanc, J. B. White and P. F. Bernath, *J. Mol. Spectrosc.* **164**, 574–579 (1994).